



Optimization of *Rhodomonas* sp. under continuous cultivation for industrial applications in aquaculture



P.C. Oostlander^{a,b,*}, J. van Houcke^b, R.H. Wijffels^{a,c}, M.J. Barbosa^a

^a Bioprocess Engineering, Wageningen University, AlgaePARC, P.O. Box 16, 6700 AA Wageningen, the Netherlands

^b Research group Aquaculture, HZ University of Applied Sciences, Edisonweg 4, 4382 NW Vlissingen, the Netherlands

^c Faculty of Biosciences and Aquaculture, Nord University, N-8049 Bodø, Norway

ARTICLE INFO

Keywords:

Rhodomonas sp.
Biomass production rate
Biomass yield on light
Turbidostat production
Growth parameter optimization
Fatty acid composition

ABSTRACT

The microalgae species *Rhodomonas* sp. is commonly used in aquaculture for its high nutritional value due to the eicosapentaenoic acid (EPA) and docosahexaenoic acid (DHA) content. Understanding the effect of cultivation parameters on biomass production rate and composition is presently limited, however essential in further commercialization of this strain. Under nutrient replete conditions, light intensity and temperature are the main factors determining biomass growth and composition. Therefore, the combined effect of light and temperature on the biomass production rate and biomass composition of *Rhodomonas* sp. was studied using a statistical Design of Experiment approach. *Rhodomonas* sp. was cultivated under continuous (turbidostat) conditions in lab-scale reactor systems (1.8 l) under different temperature (15–20–25–30 °C) and light conditions (60–195–330–465–600 $\mu\text{mol m}^{-2} \text{s}^{-1}$). Stable biomass production was observed under all conditions except experiments performed at 30 °C, which led to cell death. Under optimized growth conditions, high growth rates ($> 1.0 \text{d}^{-1}$) and high biomass production rates, up to $1.5 \text{g l}^{-1} \text{d}^{-1}$, were obtained in this study. The biomass production rate reported here is > 10 -fold higher than values reported in literature on *Rhodomonas* sp. The optimal temperature for maximal growth was found at $T = 22\text{--}24$ °C under all light conditions. The maximum biomass yield on light ($Y_{x,\text{ph}} - 0.87 \text{g mol}^{-1}$) was found at light levels between 110 and 220 $\mu\text{mol m}^{-2} \text{s}^{-1}$. The fatty acid profile was only significantly influenced by temperature, with higher EPA and DHA contents at lower temperatures (15 °C). A total fatty acid (TFA) content of 8–10% of the total dry-weight was found for all tested conditions. The EPA content fluctuated between 9 and 16% of TFA and DHA content between 6 and 9% of TFA, only affected by temperature. A maximum EPA + DHA production rate of $114 \text{mg l}^{-1} \text{d}^{-1}$ was obtained at 20 °C and high light ($600 \mu\text{mol m}^{-2} \text{s}^{-1}$) conditions.

1. Introduction

The microalgae *Rhodomonas* sp. is an important species in the aquaculture industry. It is used mainly as feed for copepod production, a live feed in aquaculture. *Rhodomonas* sp. has been shown to increase egg production, growth and survival rate of copepods [1,2]. The biomass composition and specifically the eicosapentaenoic acid (EPA) and docosahexaenoic acid (DHA) content of *Rhodomonas* sp. are often mentioned as key factors for using this algae in aquaculture applications [3,4]. Despite the importance of *Rhodomonas* sp. for aquaculture, the growth parameters have not been well characterized or optimized.

Rhodomonas sp. is described as difficult to maintain and unpredictable in mass cultivation [2].

A better understanding of the strain and the production process could greatly increase the use of *Rhodomonas* sp. in aquaculture. A significant improvement of biomass production rate and robustness is the first step towards more stable production of *Rhodomonas* sp. for aqua feed applications. This requires a better understanding of the effect of cultivation parameters (light and temperature) on the biomass yield on light, biomass production rate and the biomass composition, specifically the fatty acid composition.

Large-scale algae production aims at light limited production of

Abbreviations: C_x , Biomass concentration (g l^{-1}); D , Daily dilution rate (d^{-1}); DHA, docosahexaenoic acid; EPA, eicosapentaenoic acid; I_{ph} , Incident light intensity ($\mu\text{mol}_{\text{ph}} \text{m}^{-2} \text{s}^{-1}$); MUFA, Mono unsaturated fatty acid; PUFA, Poly unsaturated fatty acid; r_{ph} , Volumetric photon supply rate ($\text{mol}_{\text{ph}} \text{l}^{-1} \text{d}^{-1}$); r_x , Volumetric biomass production rate ($\text{g l}^{-1} \text{d}^{-1}$); SFA, Saturated fatty acids; TFA, Total fatty acid content of the biomass; V_{dilution} , Daily dilution volume (l); V_{reactor} , Total reactor volume (l); $Y_{x,\text{ph}}$, Biomass yield on light ($\text{g}_x \text{mol}_{\text{ph}}^{-1}$)

* Corresponding author at: Bioprocess Engineering Group, Wageningen University & Research, PO Box 16, 6700 AA Wageningen, the Netherlands.

E-mail address: Pieter.oostlander@wur.nl (P.C. Oostlander).

<https://doi.org/10.1016/j.algal.2020.101889>

Received 11 November 2019; Received in revised form 19 March 2020; Accepted 19 March 2020

Available online 11 April 2020

2211-9264/ © 2020 The Authors. Published by Elsevier B.V. This is an open access article under the CC BY license

(<http://creativecommons.org/licenses/by/4.0/>).

algae while optimizing the biomass yield on light for maximum biomass production rates. In a light limited situation, the cultivation temperature and the available light will determine the maximum growth rate. Temperature and light are therefore the most relevant parameters to investigate for industrial cultivation of microalgae, assuming non-limiting conditions for all other growth parameters. It is therefore required that no nutrients are limiting during cultivation. This means that all macronutrients (nitrogen, phosphorus and CO₂) as well as trace-minerals are supplied in sufficient concentrations at all times of a given cultivation.

Although the effect of light and temperature on the growth rate of *Rhodomonas* sp. has been described in literature before [5–10], most literature does not describe biomass production rates or biomass yield on light. In addition, the growth rates reported in literature are very different for similar temperatures and light intensities. This might be due to the fact that most studies are performed in shake-flask batch experiments with very limited or no control of cultivation parameters such as nutrients and pH (CO₂). Often these experiments are performed in the nutrient limited f/2 culture medium. Moreover, these studies are performed under very low light conditions with over 80% of the data found in literature working with light intensities lower than 120 $\mu\text{mol m}^{-2} \text{s}^{-1}$ [9–11]. The temperatures described in literature range from 5 to 35 °C [5,8,12] with most work focusing at 19–20 °C [6,13–16]. Evaluation of available data on *Rhodomonas* sp. in literature indicates a high probability that light is often not the limiting growth factor in these studies. Growth rates for experiments described at a temperature of 20 °C and a light intensity of $100 \pm 10 \mu\text{mol m}^{-2} \text{s}^{-1}$ vary between 0.23 d⁻¹ and 0.72 d⁻¹ [7,8,10,16,17]. The large spread of growth rates, yields uncertainty for further implementation at large scale. The large fluctuations of data could as well partially be due to a result of the use of different strains as not all studies use the same strain. A standard for *Rhodomonas* sp. in research has not been established. However, two studies comparing up to five different strains under identical conditions per study showed no differences in growth between different strains of *Rhodomonas* sp. [7,18].

Batch experiments in shake flasks are difficult to translate to industrial applications where most production is done using photobioreactors under continuous operation and controlled conditions. Data on continuous production of *Rhodomonas* sp. in photobioreactors is very limited in literature. Only two recent studies describe *Rhodomonas* sp. in larger scale reactor systems under continuous conditions in highly controlled artificial light conditions [18,19] and one study reports a lab scale system with continuous conditions [20]. Thoisen et al. [18] describe a tubular photobioreactor setup (200 l) operating continuously with fixed biomass concentrations between 0.5 and 2.0×10^6 cells ml⁻¹ at growth rates of 0.28 and 0.52 d⁻¹ producing approximately 0.02–0.08 g l⁻¹ d⁻¹. Vu et al. [19] describe a bubble-column (84 l) for *Rhodomonas* production with a concentration of 2.4×10^6 cells ml⁻¹ with a dilution rate of 0.46 d⁻¹ achieving an average production rate of about 0.11 g l⁻¹ d⁻¹ under continuous operation. Studies with other algal species grown under continuous operation at pilot scale outdoors show much higher biomass production rates. Data of de Vree for chemostat and turbidostat operation of tubular reactors showed an average biomass production rate of 0.57 g l⁻¹ d⁻¹ up to 0.90 g l⁻¹ d⁻¹ using *Nannochloropsis* sp. under Dutch climate conditions [21,22]. A pilot-scale experiment in Spain described in a study by Acien et al. [23] showed a biomass production rate of 0.3–0.7 g l⁻¹ d⁻¹ depending on the solar irradiance variations over a year for *Scenedesmus* sp. The large difference in volumetric biomass production rate between algae found in literature and currently available data for *Rhodomonas* sp. could indicate a large potential for improvement of the production of *Rhodomonas* sp. in industrial settings with optimized growth conditions.

This study aims to determine the combined effect of light intensity and cultivation temperature under continuous operation of *Rhodomonas* sp. using a larger range of conditions than described in literature. To characterize the effect of these growth parameters of *Rhodomonas* sp.,

the alga was grown in highly-controlled lab-scale flat-plate photobioreactors under continuous (turbidostat) conditions. A Design of Experiment approach was applied using a D-optimal design for the selection of experimental conditions. The design space was selected to contain light conditions between 60 and 600 $\mu\text{mol m}^{-2} \text{s}^{-1}$ and temperatures between 15 and 30 °C. The growth rate, biomass production rate and biomass yield on light as well as the fatty acid composition are determined for each combination of temperature and light.

2. Materials and methods

2.1. Strains, cultivation medium and pre-culture conditions

Rhodomonas sp. was provided by the Dutch aquaculture industry, as being one of the strains used in commercial applications. The strain was characterized by 18S sequencing and confirmed to be *Rhodomonas* sp. (data not shown). Pre-cultures of *Rhodomonas* sp. were maintained in 250 ml Erlenmeyer flasks with 100 ml culture volume. Flasks were placed in an orbital shaker (100 rpm) maintained at 25 °C and low light conditions ($50 \pm 10 \mu\text{mol m}^{-2} \text{s}^{-1}$) applied 24 h per day. The headspace was enriched with 2.5% CO₂ for pH control maintaining a pH of 8.0 ± 0.5 . Cultures were used for the inoculation of experimental reactors after 10 days of batch cultivation in flasks. The growth media used was based on the L1-medium with an adjusted iron source [24]. Artificial seawater was used in all experiments. All nutrients were added in higher concentration than the L1-media to prevent limitations. FeCl₃ was substituted by lower concentrations (27.8 $\mu\text{mol l}^{-1}$) of Na-FeEDTA to prevent precipitation. The complete growth medium and the artificial seawater contained final concentrations of: NaCl 420 mM; NaNO₃ 17.6 mM; Na₂SO₄ 22.5 mM; MgCl₂ * 6H₂O 48.2 mM; CaCl₂ * 2H₂O 3.6 mM; K₂SO₄ 4.9 mM; NaH₂PO₄ * H₂O 0.7 mM; Na-FeEDTA 27.8 μM ; Na₂EDTA 0.30 mM; MnCl₂ * 4H₂O 14.3 μM ; ZnSO₄ * 7H₂O 1.5 μM ; CoCl₂ * 6H₂O 0.8 μM ; CuSO₄ * 5H₂O 0.2 μM ; Na₂MoO₄ * 2H₂O 1.6 μM ; H₂SeO₃ * 2H₂O 0.2 μM ; NiSO₄ * 6H₂O 0.2 μM ; Na₃VO₄ 0.2 μM ; K₂CrO₄ 0.2 μM ; Vitamin B1 7.5 μM ; Vitamin H 0.04 μM ; Vitamin B12 0.1 μM . The same growth media was used in reactor experiments and shake flasks with the exception of 20 mM HEPES (4-(2-hydroxyethyl)piperazine-1-ethanesulfonic acid) and 10 mM NaHCO₃, which were added as a pH buffer to flask cultures only. The pH of the growth medium was adjusted with NaOH to pH 7.5 and the media was filter sterilized prior to use (Sartobran 300 – pore size 0.2 μm).

2.2. Photobioreactor operation and experimental setup

Experiments were performed in an aseptic, heat-sterilized, flat-panel, photobioreactor (Labfors 5 Lux, Infors HT, Switzerland) with a total culture volume of 1.8 l. Mixing was applied by aeration of the culture with 900 ml min⁻¹ filtered air (0.2 μm). CO₂ was injected on-demand to the airflow for pH control, with the pH maintained at pH 7.5. Culture temperature was controlled at the selected value for each experiment (15–20–25–30 °C) by recirculation of water through a water jacket in direct contact with the cultivation chamber of the reactor. The incident light intensity was provided by the integrated LED-light system of the Labfors 5 Lux. The 260 LED lights, evenly distributed over the reactor were calibrated and the incident light intensity was set at the selected values for each experiment and supplied 24 h per day (60–195–330–495–600 $\mu\text{mol m}^{-2} \text{s}^{-1}$). Reactors were inoculated at a starting OD₇₅₀ of 0.15 ± 0.02 with *Rhodomonas* cultures from shake flasks. Reactor operation started with a batch phase, operated with a luminostat for light control, until the desired biomass concentration and light level were achieved for continuous operation. Not every experiment started from flask cultures, some experiments were started from a steady-state of a previous experiment by changing the reactor settings to new conditions for temperature and light. During continuous operations in turbidostat mode, on-demand dilution was applied to

maintain the light at the backside of the reactor at the set-point ($15 \mu\text{mol m}^{-2} \text{s}^{-1}$) measured by the integrated light sensor (LI-250, Licor, USA). Under continuous dilution and constant conditions, the growth rate of the microalgae is equal to the dilution rate of the reactor under steady state. Reactors were sampled daily and operated until a steady-state was obtained under the turbidostat conditions before sampling for analysis of the fatty acid composition. Steady state was defined when the total dilution volume was equal to three times the reactor volume with unchanged biomass concentration and dilution rate over the time required to reach this dilution volume. Depending on the experimental settings, a steady-state was achieved between 10 and 15 days after the start of an experiment and required 3–6 days of stable conditions in the reactor system.

2.3. Experimental design

A Design of Experiment approach was used to select the experiments to be performed within the selected design space. The design space consists of a 2-factor design using 5 levels for each factor. The first factor is light intensity with values between 60 and $600 \mu\text{mol m}^{-2} \text{s}^{-1}$. The second factor is cultivation temperature (15–30 °C). A D-optimal design was selected as created using the Umetrics MODDE 9.1 software package. This method was applied to minimize the required reactor runs while maximizing data output. The D-optimal design consists of a total of 15 experiments. The centre point of the D-optimal design ($I_{\text{ph}} = 330 \mu\text{mol m}^{-2} \text{s}^{-1}$ and $T = 20 \text{ °C}$) was operated in 3 separate experiments. One of the experimental settings was performed in duplicate ($I_{\text{ph}} = 60 \mu\text{mol m}^{-2} \text{s}^{-1}$ and $T = 15 \text{ °C}$), with all other experimental settings only performed once, according to the D-optimal design. Using this approach, a total of 12 different experimental conditions were measured. A list of all experiments and corresponding settings for temperature and light can be found in Table 1. With no growth at 30 °C (see Section 3) the additional use of a growth temperature of 27.5 °C was tested.

2.4. Measurements (growth, biomass production rate, biomass yield on light and fatty acid composition)

Daily samples were taken from each reactor to monitor culture growth. Biomass concentration, growth rate and biomass yield on light were determined daily. Data of four experiments in steady-state is represented in Supplementary files B.

Biomass concentration was determined by OD-measurements and cell-counts. Dry-weight was only determined at steady-state. A 2.0 ml sample was taken daily directly from the reactor volume. The optical density was determined, in duplicate, at 750 nm using a UV-VIS spectrophotometer (Hach Lange DR-6000, light path 1 cm). Cell count was determined, in duplicate, with a Multisizer II (Beckman Coulter) using a 50 μm aperture tube after diluting the sample using the original growth medium. Growth medium was applied rather than Isotone as the latter influences cell size for *Rhodomonas* sp. during the analysis (data not shown).

Table 1

Experimental conditions and results growth of *Rhodomonas* sp. under different combinations of temperature and light intensities. All values represent measurements during steady-state. Biomass concentration represented the calculated biomass concentration as based on the Eq. (3).

Temperature	°C	15	15	15	15	20	20	20	20	20	25	25	25	27.5	30
Light intensity	$\mu\text{mol m}^{-2} \text{s}^{-1}$	60	60	465	600	195	330	330	330	600	60	330	600	60–195–330	60–195–465
Biomass concentration	g l^{-1}	0.19	0.18	1.37	1.59	0.75	1.06	1.03	1.04	1.41	0.36	0.99	1.41	–	–
	Cells ml^{-1} (millions)	1.65	1.53	10.54	12.18	5.78	8.32	7.83	7.82	11.32	2.98	7.64	11.25	–	–
Growth rate	μ (d^{-1})	0.59	0.56	0.65	0.55	0.90	0.97	1.01	0.97	0.94	0.43	1.10	1.02	–	–
Biomass production rate	Rx ($\text{g l}^{-1} \text{d}^{-1}$)	0.11	0.10	0.87	0.87	0.68	1.03	1.06	1.01	1.35	0.15	1.10	1.44	–	–
Biomass yield on light	$Y_{\text{x,ph}}$ (g mol^{-1})	0.59	0.51	0.45	0.34	0.88	0.76	0.78	0.74	0.53	0.79	0.81	0.57	–	–

In steady-state the growth rate is equal to the dilution rate and is described by Eq. (1). The daily dilution rate (D) was determined by the mass decrease of the fresh medium vessel for inflow of medium between two measurements (V_{dilution}) and the total reactor volume (V_{reactor}) [25]. The vessel was placed on a balance and logged continuously.

$$\mu = D = \frac{V_{\text{dilution}}}{V_{\text{reactor}}} \quad (1)$$

The biomass yield on light ($Y_{\text{x,ph}}$ in g mol^{-1}) is calculated based on the daily dilution rate (D in d^{-1}), the biomass concentration in the reactor system (C_x in g l^{-1}) and the volumetric photon supply rate (r_{ph} in $\text{mol}_{\text{ph}} \text{l}^{-1} \text{d}^{-1}$) according to Eq. (2) [26].

$$Y_{\text{x,ph}} = \frac{D * C_x}{r_{\text{ph}}} \quad (2)$$

Rhodomonas sp. does not contain a cell wall making the cells too fragile for conventional dry-weight methods where cells are filtered and washed with ammonium formate on a filter. An adapted dry-weight protocol was established for dry-weight determination of *Rhodomonas* sp. in this study. The dry weight of the biomass was determined in triplicate by collecting a 10.0 ml sample in a pre-dried and weighed glass tube. Cells were collected by centrifugation (10 min at 1200 rcf), the supernatant was stored for nutrient analysis and the pellet was washed by re-suspending in ammonium-formate (0.55 M). Cell was collected by centrifugation (10 min at 1200 rcf) and supernatant was discarded. The glass tube containing the washed cell-pellet was dried, for at least 24 h, to a stable weight in a stove at 100 °C to determine the final dry weight. A correlation between OD_{750} and the measured dry weight for all experiments was used for the estimation of dry weight at other time-points during the experiments. The OD-DW correlation is given in Eq. (3) (also see Supplementary files A) where DW is the dry-weight of the sample in g l^{-1} and OD_{750} is the optical density at 750 nm measured according to the above described method.

$$\text{DW} = 0.7236 * \text{OD}_{750} - 0.0205 \quad (3)$$

2.5. Fatty acid analysis

Samples for fatty acid analysis were collected and prepared according to Breuer et al. using sample preparation method 1.1 and stored at -20 °C until extraction [27]. Fatty acid extraction and quantification was performed in duplicate for each reactor as based on the method as described by Breuer et al. [27]. The method was slightly adjusted as *Rhodomonas* sp. did not require extended cell disruption steps. In short: cells are disrupted by bead-beating and transferred to a glass tube using chloroform containing C_{15} -TAG internal standard. Chloroform was evaporated from the tube by a nitrogen gas stream. Fatty acids were methylated by incubation with methanol/ H_2SO_4 (5%) at 70 °C for 3 h and extracted using hexane. The fatty acids in the hexane phase were identified and quantified by gas chromatography (GC-FID) as described by Breuer et al. with the exception that the oven temperature was maintained at 200 °C for 54 min to allow for EPA and DHA separation

and detection [27].

2.6. Data analysis

Data processing and visualization for growth rate, biomass production rate and biomass yield on light was performed in SigmaPlot V10.0. Contour plots are created to depict the results in 2D, showing the trends of each of the results as a function of temperature and light intensity. Only data of successful steady-state experiments is used for data analysis. For biomass yield on light data; SigmaPlot V10.0 was used to plot a regression and describe biomass yield on light as a function of the cultivation temperature and light intensity. All data used for regressions follow a normal distribution. The presented trends for growth rate, biomass yield on light and fatty acid composition cannot be extrapolated beyond the upper temperature limit given in the graphs. Observed trends might be extrapolated for higher light levels or lower temperatures, but have not been tested in our study. Statistical analysis of fatty acid data was performed using a two-tailed two-sample equal variance Student's *t*-test in Microsoft Excel.

3. Results and discussion

All experiments showed stable and reproducible results under all conditions except for the experiments performed at 30 °C. No biofilm or fouling was observed for any of the experiments under steady state conditions. For experiments performed at 30 °C growth decreased daily until no growth was observed. As a result, no steady state could be obtained for conditions at 30 °C, similar behavior was found for reactors operated at 27.5 °C (data not shown). All other temperature conditions (15–20–25 °C) did show good growth and resulted in stable turbidostat operations. It is therefore concluded that *Rhodomonas* sp. cannot be cultivated under continuous conditions at 27.5 °C or above. The maximum temperature for *Rhodomonas* sp. should be between 25.0 and 27.5 °C but was not determined in this study. This inability to grow at higher temperatures is an unexpected result as literature describes growth studies with *Rhodomonas* sp. at 29 °C up to 33 °C [5,7,28,29]. In our results, no immediate cell death was observed but the growth rate decreased daily over a 4–7 day period until growth stopped completely. All studies in literature reporting growth rates at higher temperatures were performed under batch culture conditions. With multiple days of a daily decreasing growth rate, a measurement for growth rate is possible under batch culture conditions when only measured at two time points but this growth behavior does not allow for a steady-state measurement under continuous conditions.

The center point of the D-optimal design ($T = 20$ °C and $I_{ph} = 330$ $\mu\text{mol m}^{-2} \text{s}^{-1}$) shows highly reproducible results as indicated by the small deviation found between the three biological replicates. For the three biological replicates, a biomass concentration of 1.05 ± 0.02 g l^{-1} was found with a growth rate of 0.98 ± 0.02 d^{-1} resulting in a biomass production rate of 1.03 ± 0.02 $\text{g l}^{-1} \text{d}^{-1}$ and a biomass yield on light of 0.76 ± 0.02 g mol^{-1} . The duplicate experiment ($T = 15$ °C and $I_{ph} = 60$ $\mu\text{mol m}^{-2} \text{s}^{-1}$) shows slightly larger deviations between the two duplicate experiments at steady-states. This larger deviation is attributed to technical challenges associated to the very low incident light levels (60 $\mu\text{mol m}^{-2} \text{s}^{-1}$) in the turbidostat mode. A biomass concentration of 0.18 ± 0.02 g l^{-1} was obtained with a growth rate of 0.57 ± 0.02 d^{-1} during steady state. This resulted in a biomass production rate of 0.11 ± 0.01 $\text{g l}^{-1} \text{d}^{-1}$ with a biomass yield on light of 0.55 ± 0.06 g mol^{-1} . The results of the replicate experiments and the center point indicated good reproducibility of all tested conditions also for conditions further away from the center of the experimental design.

3.1. Biomass concentration, growth rate and biomass production rate

A contour plot of the biomass concentration is shown in Fig. 1A. The

results show that the biomass concentration is almost exclusively affected by light intensity showing a positive correlation between light intensity and biomass concentration. This correlation is the direct result of the turbidostat settings as applied in the experiments. A higher incident light intensity with equal outgoing light in all experiments results in a higher biomass concentration.

The contour plot of Fig. 1B shows the growth rate. It can be seen that both temperature and light intensity have a large effect on the observed growth rate. An optimum growth rate seems to be found within the tested limits for the two conditions for light at $300\text{--}500$ $\mu\text{mol m}^{-2} \text{s}^{-1}$ and a temperature of $23\text{--}25$ °C. The experiments closest to this optimum were performed at 25 °C with 330 and 600 $\mu\text{mol m}^{-2} \text{s}^{-1}$ with growth rates of 1.10 and 1.02 d^{-1} , respectively. The effect of temperature on growth is clearly observed when comparing data of experiments at all different temperatures for high light conditions (600 $\mu\text{mol m}^{-2} \text{s}^{-1}$). An increased growth rate is found for increased temperatures from 15 °C (0.55 d^{-1}) to 20 °C (0.94 d^{-1}) and 25 °C (1.02 d^{-1}). The maximum growth rate for experiments at 15 °C did not exceed 0.65 d^{-1} regardless of the applied light intensity. All experiments at 15 °C showed very similar growth rates of 0.60 ± 0.05 d^{-1} with almost no effect of light intensity. This indicates that under lower temperature conditions the growth of *Rhodomonas* sp. is limited by temperature rather than by light intensity. A clear effect of light intensity on the observed growth rate is found for higher temperature conditions at 25 °C with the maximum observed growth rate of 1.10 d^{-1} under higher light conditions (> 330 $\mu\text{mol m}^{-2} \text{s}^{-1}$) compared to the lower values found under lower light conditions (0.43 d^{-1} at 60 $\mu\text{mol m}^{-2} \text{s}^{-1}$). It has to be noted that even though the data could suggest higher growth rates at even higher temperatures, this is not the case as *Rhodomonas* sp. did not show stable growth at 27.5 °C and 30 °C in our experiments. The maximum growth rate found in our study is higher than most values described in literature. Only batch cultivations are described in literature, which means that other factors than light and temperature might be limiting the growth rate. Most studies, including very recent work, on *Rhodomonas* sp. describe maximum observed growth rates between 0.5 and 0.75 d^{-1} [6,11,16,17]. Higher growth rates, similar to the maximum value found in our study are reported in some studies but only for a short period (1 or 3 days) in batch cultivation under very dilute culture conditions [9,10]. The consistent high growth rates under continuous cultivation conditions has never been described before.

The biomass production rate (r_x in $\text{g l}^{-1} \text{d}^{-1}$) was calculated from the growth rate (μ) and biomass concentration (C_x) and is shown in Fig. 1C. The biomass concentration is mostly affected by light intensity; growth rate is positively affected by both light and temperature. Therefore, the biomass production rate also shows a positive influence from both temperature and light. Higher temperatures and higher light conditions result in higher biomass production rates within the given boundaries for temperature. The effect of temperature is mostly observed at higher light intensities (> 300 $\mu\text{mol m}^{-2} \text{s}^{-1}$) where a 65% higher biomass production rate is found for the $T = 25$ °C $I_{ph} = 600$ $\mu\text{mol m}^{-2} \text{s}^{-1}$ (1.44 $\text{g l}^{-1} \text{d}^{-1}$) compared to $T = 15$ °C $I_{ph} = 600$ $\mu\text{mol m}^{-2} \text{s}^{-1}$ (0.87 $\text{g l}^{-1} \text{d}^{-1}$), in similarity to the results for growth rate. No optimum is found for biomass production rate within the tested levels of light and temperature. Light conditions higher than those tested here will result in increased biomass production rate until photo inhibition occurs. Photo inhibition was not observed within the tested conditions in this study.

Very limited literature on *Rhodomonas* sp. under continuous cultivation conditions is available. Biomass production rates available in literature range between 0.02 and 0.11 $\text{g l}^{-1} \text{d}^{-1}$ but were all obtained in large pilot-scale systems, which are more difficult to control. Patil et al. [20] did describe a 1.8 l lab-scale reactor with a production rate of 0.09 $\text{g l}^{-1} \text{d}^{-1}$ in turbidostat mode under low light conditions. These results show that we were able to achieve a > 10 -fold increase, with 1.4 $\text{g l}^{-1} \text{d}^{-1}$, for *Rhodomonas* sp. under continuous cultivation

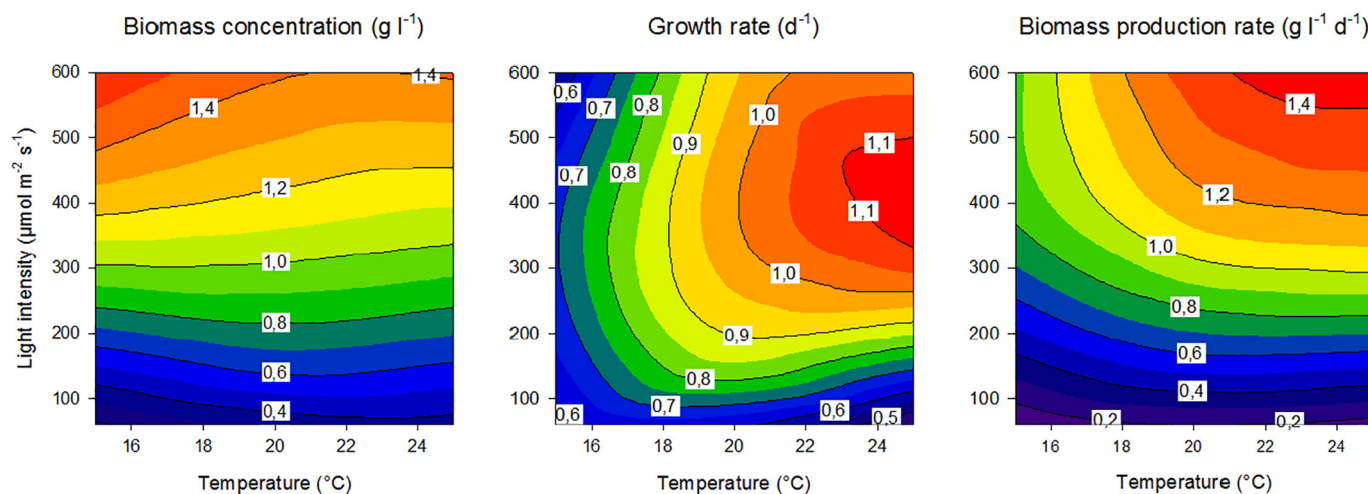


Fig. 1. Experimental results for biomass concentration (panel A - g l^{-1}), growth rate (panel B - d^{-1}) and biomass production rate (panel C - $\text{g l}^{-1} \text{d}^{-1}$) as a function of temperature (x-axis - $^{\circ}\text{C}$) and light intensity (y-axis - $\mu\text{mol m}^{-2} \text{s}^{-1}$) represented as 2D-countour plots.

conditions. This large increase in biomass production rate compared to common practice found in literature is a very significant improvement for *Rhodomonas* sp. as a production strain for aquaculture.

The production rate of some other well-known microalgae strains for aquaculture application such as *Nannochloropsis* sp. and *Tetraselmis* sp. have been described in literature before. Pilot scale studies of *Nannochloropsis* sp. under outdoor conditions showed production rates of $0.60 \text{ g l}^{-1} \text{d}^{-1}$ and $0.90 \text{ g l}^{-1} \text{d}^{-1}$ [21,22]. A lab scale screening study of multiple species of *Nannochloropsis* described biomass production rates up to $0.766 \text{ g l}^{-1} \text{d}^{-1}$ [30]. *Tetraselmis* sp. has a described production rate of around $0.50 \text{ g l}^{-1} \text{d}^{-1}$ under outdoor pilot-scale production [31]. *Phaeodactylum tricorntutum* in literature has been described with biomass production at pilot scale of about $0.20 \text{ g l}^{-1} \text{d}^{-1}$ using Norwegian sunlight conditions [32] and up to $1.38 \text{ g l}^{-1} \text{d}^{-1}$ in a different study [33]. At lab scale *P. tricorntutum* showed a biomass production rate of $0.68 \text{ g l}^{-1} \text{d}^{-1}$ at relatively low light conditions ($260 \mu\text{mol m}^{-2} \text{s}^{-1}$) [34]. *Isochrysis* sp. was described with production rates of about $0.50 \text{ g l}^{-1} \text{d}^{-1}$ under semi continuous lab experiments [35] A literature study performed under very similar culture conditions (30°C and $500 \mu\text{mol m}^{-2} \text{s}^{-1}$) in the same lab scale reactor as described in our study showed a biomass production rate of $1.3 \text{ g l}^{-1} \text{d}^{-1}$ compared to $1.4 \text{ g l}^{-1} \text{d}^{-1}$ for *Rhodomonas* sp. at 25°C and $600 \mu\text{mol m}^{-2} \text{s}^{-1}$ using *Neochloris oleoabundans* [36]. The results with *Rhodomonas* sp. in our study show that the biomass production rate of *Rhodomonas* sp. can be equal to other microalgae species for aquaculture under optimized growth conditions.

3.2. Biomass yield on light

The biomass yield on light represents the efficiency of light conversion into biomass. Fig. 2 shows the biomass yield on light (z-axis) as a function of the temperature (x-axis) and light intensity (y-axis). The experimental data is displayed as black dots. A Gaussian regression showed the best fit through all data-points and is depicted with the 3D-field in Fig. 2. The regression has an R^2 of 0.97 passing all statistical tests. From this regression, the optimal conditions and maximum values for biomass yield on light were calculated. The predicted maximum biomass yield on light for *Rhodomonas* sp. is calculated at 0.87 g mol^{-1} for temperatures between 22 and 24°C with light intensities between 110 and $220 \mu\text{mol m}^{-2} \text{s}^{-1}$. The results for biomass yield on light clearly show a negative correlation between the biomass yield on light and the light intensity. This correlation is expected and has been described in literature before at different scales [21,22,36].

Comparison of the biomass yield on light for *Rhodomonas* sp. from

this study with other, more commonly used, algae species in literature shows that *Rhodomonas* sp. performs very similar to other algae strains. De Winter found a biomass yield on light of 0.66 g mol^{-1} for *Neochloris oleoabundans* at 30°C and $500 \mu\text{mol m}^{-2} \text{s}^{-1}$ using the same lab scale reactor [36]. The regression shows a predicted biomass yield on light for *Rhodomonas* sp. of 0.65 g mol^{-1} at equal light conditions at 25°C .

The negative impact of lower temperatures on *Rhodomonas* sp. as found for growth rate and biomass production rate is also clearly found for the biomass yield on light. A predicted 33–40% reduction of biomass yield on light was calculated at 15°C compared to 24°C , at equal light conditions. The effect of temperature on biomass yield on light increases with increasing light intensities, indicating the need to grow *Rhodomonas* sp. at 22 – 24°C for maximized biomass yield on light. The optimum light intensity for biomass yield on light is higher (110 – $220 \mu\text{mol m}^{-2} \text{s}^{-1}$) than what is used in most literature (mostly 20 – $80 \mu\text{mol m}^{-2} \text{s}^{-1}$) on *Rhodomonas* sp., suggesting that studies performed under these low light conditions are performed under sub-optimal light conditions. This could explain the low growth rates are described for *Rhodomonas* sp. in literature [2,37,38]. It has to be noted that although the highest biomass yield on light is found at 110 – $220 \mu\text{mol m}^{-2} \text{s}^{-1}$, these conditions will not lead to the most optimized *Rhodomonas* sp. production at large scale due to the relatively low biomass production rates found at these light levels as can be seen from data for biomass production rate (Fig. 1C).

3.3. Fatty acid composition

The fatty acid composition of *Rhodomonas* sp. in all experimental conditions is summarized in Fig. 3, detailed results of total fatty acid composition are shown in Table 2. The total fatty acid content (TFA) of *Rhodomonas* sp. in all experiments fluctuates between 78 and 95 mgFA gDW^{-1} . A significant effect of the cultivation temperature on the total fatty acid content ($P < 0.05$) and composition ($P < 0.05$) was found whereas light intensity did not show a significant effect on the fatty acid content or composition. Fig. 3 represents the average fatty acid composition and profile of *Rhodomonas* sp. for all experiments performed under equal temperatures. The error bars depict the standard deviation of all experimental conditions (varying light intensities) with the given cultivation temperature. The fatty acid profiles are summarized in four categories of fatty acids; saturated fatty acids (SFA) mono-unsaturated fatty acids (MUFA) poly unsaturated fatty acids (PUFA) excluding eicosapentaenoic acid (C20:5 - EPA) and docosahexaenoic acid (C22:6 - DHA) and EPA with DHA as a separate category (EPA + DHA). The fatty acid profiles show a high degree of unsaturation for all

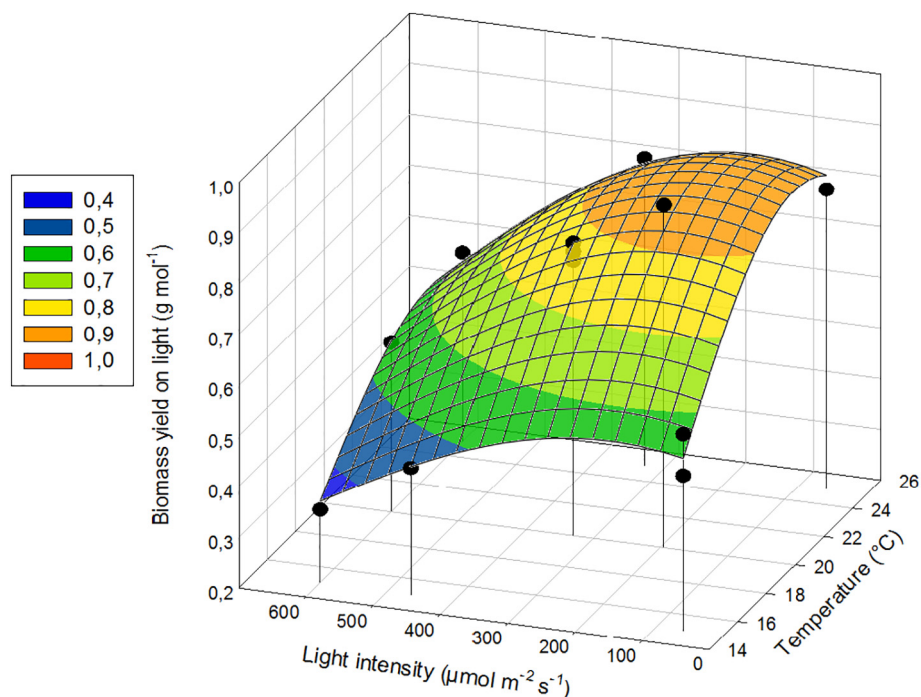


Fig. 2. Biomass yield on light (z-axis - g mol^{-1}) as a function of light intensity (x-axis - $\mu\text{mol m}^{-2} \text{s}^{-1}$) and temperature (y-axis - $^{\circ}\text{C}$). Black dots: measurements of individual experiments. 3D-field: Gaussian regression through all datapoints.

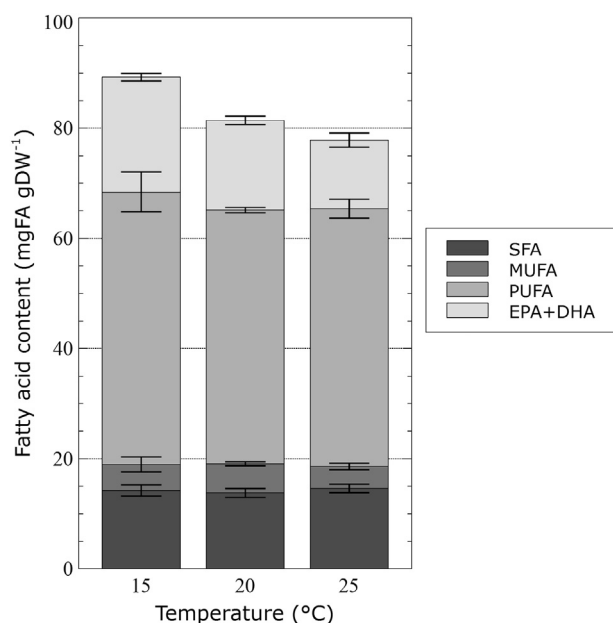


Fig. 3. Fatty acid composition of *Rhodomonas* sp. as grouped in 4 categories, SFA: Saturated fatty acids, MUFA: mono-unsaturated fatty acids, PUFA: poly unsaturated fatty acids excluding eicosapentaenoic acid (EPA) and docosahexaenoic acid (DHA) and a separate category for EPA + DHA. Values depict the average over all experiments of the same temperature but performed under different light intensities (15 $^{\circ}\text{C}$ n = 4, 20 $^{\circ}\text{C}$ n = 5, 25 $^{\circ}\text{C}$ n = 3) error bars show the deviation between samples of different light intensities.

temperatures with a total 72–80% of TFA found as PUFAs and EPA + DHA. The content of EPA ranges between 9 and 16% of TFA and the DHA between 6 and 9% of TFA for the different temperatures. No significant changes in SFA, MUFA and PUFA are found between different temperatures or light intensities between any of the tested conditions ($P > 0.05$). The temperature shows a significant effect on the EPA + DHA fraction only ($P < 0.05$) but light does not significantly

influence this fraction ($P > 0.05$). The effect on total fatty acid content between the different cultivation temperatures is therefore exclusively the result of the change in EPA + DHA content at different temperatures. Fig. 4 summarizes the correlation for both EPA and DHA content in the biomass (mgFA gDW^{-1}) as a function of the cultivation temperature with linear regressions. The regressions have an R^2 of 0.89 and 0.90 for EPA and DHA, respectively ($P < 0.01$). A very similar distribution of the fatty acid classes, with a strong effect of temperature on the total PUFA fraction in *Rhodomonas* sp. has been described in literature [19,37–39]. However, the total fatty acid content in literature fluctuates greatly depending on culture conditions but is typically higher (150–250 mgFA gDW^{-1}) than the average of 83 mgFA gDW^{-1} found in our study. Fernandes et al. [37] describes a very comparable fatty acid composition and content and TFA content (71 mgFA gDW^{-1}) under nutrient replete conditions but shows a large effect of reduced nutrients conditions on the TFA content increasing to 150 mgFA gDW^{-1} of dry weight. The relatively low TFA-content found in our study could therefore be explained by the fast growing cells under continuous cultivation conditions compared to the TFA content found for potentially nutrient limited batch cultures described in literature [37,40]. Studies that show comparable TFA content to this study also report similar EPA and DHA content in %TFA [18,19,37,39].

A large change in PUFA composition occurs with changing temperatures (detailed results found in Table 2). Experimental conditions at 15 $^{\circ}\text{C}$ show a higher degree of unsaturation in the PUFA fraction, mainly represented in the C18:2, C18:3 and C18:4 fractions. With C18:2 increasing from $5.2 \pm 0.8\%$ to $25.4 \pm 1.0\%$ of total PUFAs from 15 $^{\circ}\text{C}$ to 25 $^{\circ}\text{C}$ experiments respectively, compared to C18:4 which decreases from $32.1 \pm 2.4\%$ of total PUFAs at 15 $^{\circ}\text{C}$ to $19.5 \pm 2.3\%$ under 25 $^{\circ}\text{C}$ conditions. Similar correlations between cultivation temperature and the fatty acid composition have been described in literature for other algae strains and cyanobacteria [41–43]. The effect of temperature on the degree of saturation has been found in multiple studies for other aquaculture related algae species such as *Isochrysis* sp. [44,45]. Aussant et al. describe a similar trend for the saturation of fatty acids as a result of growth under non-optimal temperatures for multiple algal species including *Rhodomonas salina* [46]. Hoffmann et al. describe that the

Table 2

Fatty acid content of *Rhodomonas* sp. cultivated under different combined conditions for temperature ($^{\circ}\text{C}$) and light intensity ($\mu\text{mol m}^{-2} \text{s}^{-1}$). Fatty acids are represented as mgFA gDW^{-1} and fatty acids classes give as %TFA (SFA: Saturate Fatty acids; MUFA: Monounsaturated fatty acids; PUFA: Poly-unsaturated fatty acids with EPA + DHA as a separate class).

T ($^{\circ}\text{C}$)	15	15	15	15	20	20	20	20	20	25	25	25
I _{ph} ($\mu\text{mol m}^{-2} \text{s}^{-1}$)	60	60	465	600	195	330	330	330	600	60	330	600
C12:0	0.4	0.3	0.0	0.2	0.0	0.0	0.0	0.0	0.2	0.0	0.3	0.3
C14:0	7.6	6.0	5.1	5.4	5.7	4.5	5.5	4.2	4.8	6.1	4.8	4.6
C16:0	7.0	6.3	9.8	8.8	7.5	9.5	9.1	8.3	9.3	7.5	9.3	10.6
C16:1	1.3	1.1	0.8	0.9	1.1	1.0	1.0	1.0	0.9	1.0	1.0	0.8
C16:2	0.8	0.7	0.4	0.2	1.1	0.6	0.7	0.1	0.2	2.4	0.5	0.4
C16:3	0.3	0.6	0.2	0.4	0.3	0.3	0.4	0.4	0.4	0.0	0.3	0.4
C18:0	0.0	0.0	0.1	0.1	0.0	0.1	0.1	0.0	0.1	0.0	0.1	0.1
C18:1	5.4	4.2	2.5	1.8	4.1	4.8	4.6	4.2	3.9	2.1	3.6	3.6
C18:2	3.9	2.7	4.3	3.9	5.7	6.1	6.2	5.6	5.1	15.5	14.2	15.4
C18:3	23.8	25.0	20.6	19.9	20.0	19.7	19.7	19.1	22.3	21.5	15.8	14.5
C18:4	24.0	24.4	20.2	21.6	18.7	18.3	18.2	20.3	18.6	9.8	13.0	11.9
C20:1	0.0	0.0	0.6	0.4	0.0	0.0	0.0	0.0	0.0	0.0	0.0	0.0
C20:3-n3	0.0	0.0	0.0	0.0	0.0	1.2	0.0	0.8	0.0	0.0	2.3	2.5
C20:5-n3 - EPA	13.1	13.7	12.2	13.4	9.3	9.9	9.6	9.7	10.7	5.4	7.2	8.6
C22:6 - DHA	8.4	7.5	7.4	7.7	6.0	6.6	6.5	6.3	6.9	5.5	5.1	5.5
TFA (mg gDW^{-1})	95.8	92.3	84.2	84.6	79.4	82.7	81.5	80.0	83.4	76.9	77.4	79.1
Σ SFA (%TFA)	16%	13%	16%	15%	14%	15%	15%	13%	15%	14%	15%	16%
Σ MUFA (%TFA)	7%	5%	4%	3%	5%	6%	6%	5%	5%	3%	5%	5%
Σ PUFA excl. EPA + DHA (%TFA)	55%	56%	48%	48%	48%	48%	47%	48%	49%	51%	48%	47%
Σ EPA + DHA (%TFA)	22%	22%	20%	22%	16%	17%	17%	17%	18%	11%	13%	15%

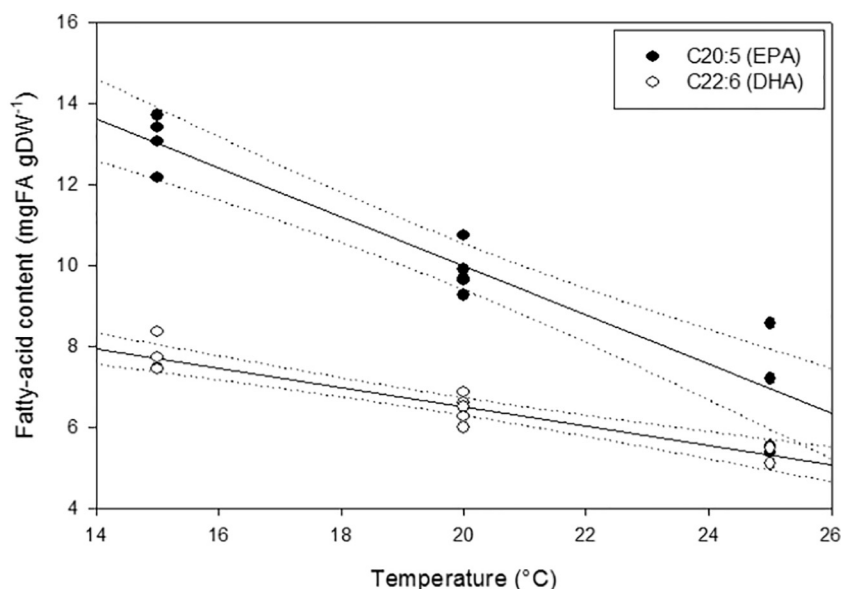


Fig. 4. Regression lines for the eicosapentaenoic acid (EPA) content (black circles) and docosahexaenoic acid (DHA) content (white circles) as a function of temperature. Circles show individual measurements of all experimental conditions. Solid line is the regression and dotted lines indicated the 95% confidence interval.

increase of TFA and degree of saturation under lower temperatures could be the result of temperature induced limited nitrogen uptake [47]. It has also been suggested that the increased content of PUFAs at low temperatures compensates for reduced membrane fluidity under lower temperatures, even though this was never proven in detail [48].

3.4. Total fatty acid and EPA + DHA production rate

The production rates ($\text{mg l}^{-1} \text{d}^{-1}$) of total fatty acids and EPA + DHA are presented in Fig. 5. The TFA-production rate (Fig. 5A) follows the same pattern as the biomass production rate with an effect of both temperature and light intensity. The highest TFA-production rate ($114 \text{ mg l}^{-1} \text{d}^{-1}$) is found at the highest temperature and light condition tested ($T = 25 \text{ }^{\circ}\text{C}$ and $I_{\text{ph}} = 600 \mu\text{mol m}^{-2} \text{s}^{-1}$). The EPA + DHA production rate shows an optimum at around $20 \text{ }^{\circ}\text{C}$, with the effect of temperature only clear at higher light intensities. The maximum EPA + DHA production rate measured in our experiments

was $24 \text{ mg l}^{-1} \text{d}^{-1}$ at $T = 20 \text{ }^{\circ}\text{C}$ and $I_{\text{ph}} = 600 \mu\text{mol m}^{-2} \text{s}^{-1}$. Even though the maximum EPA + DHA content is observed at the lowest experimental temperature of $15 \text{ }^{\circ}\text{C}$ (Fig. 4) the EPA + DHA production rate decreases at lower temperatures as a result of the lower growth rates for these temperatures (Fig. 1B). The decrease of EPA + DHA production rate at higher temperatures ($25 \text{ }^{\circ}\text{C}$) is the result of higher growth rates with a decreased EPA + DHA content in the biomass. Values for the EPA or DHA content of *Rhodomonas* sp. are available in literature but production rates under continuous cultivation conditions and the clear effect of temperature on EPA + DHA production rate have not been described before. The effect of temperature on fatty acid content and production rate described in our study could be used to effectively select culture conditions for the highest nutritional value of the biomass in aqua feed applications while achieving maximum production.

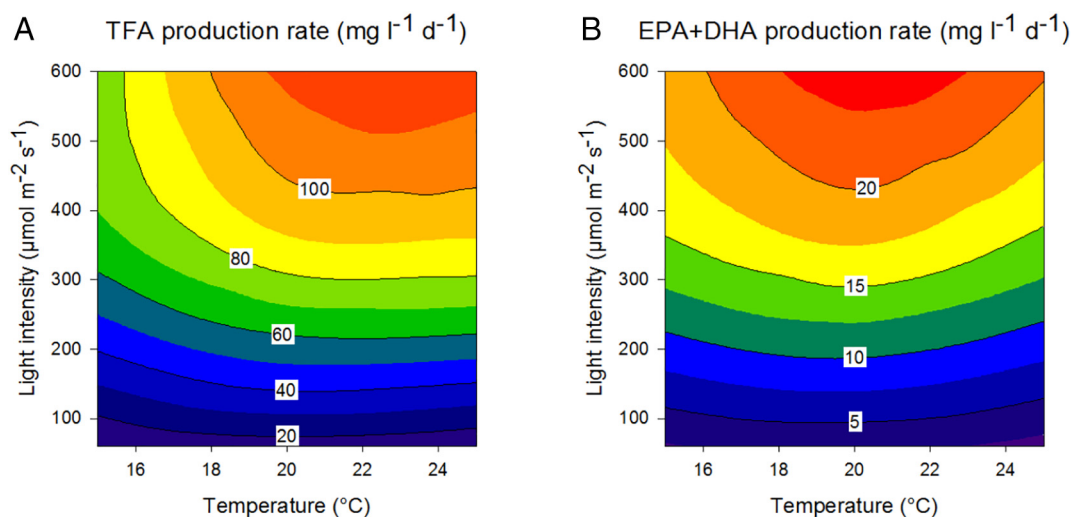


Fig. 5. TFA production rate (A) and eicosapentaenoic acid docosahexaenoic acid (EPA + DHA) production rate (B) in $\text{mg l}^{-1} \text{d}^{-1}$ plotted as a function of Temperature (x-axis $^{\circ}\text{C}$) and light intensity (y-axis - $\mu\text{mol m}^{-2} \text{s}^{-1}$).

4. Conclusion

Rhodomonas sp. was successfully cultivated under continuous conditions with stable biomass production rates and high growth rates ($> 1.0 \text{ d}^{-1}$) found at optimal conditions. The obtained biomass production rates ($0.5\text{--}1.5 \text{ g l}^{-1} \text{d}^{-1}$) show a > 10 -fold increase from values currently available in literature for *Rhodomonas* sp. This improved biomass production rate was possible due to optimization of both light and temperature without any other limitations to the culture. This optimization could be a significant step towards industrial implementation of *Rhodomonas* sp. production for aquaculture feed applications. The production rates obtainable with *Rhodomonas* sp. are comparable with more commonly used algal strains in aquaculture such as *Nannochloropsis* sp. and *Tetraselmis* sp. in similar reactor systems. The highest biomass production rate is found at temperatures of $25 \text{ }^{\circ}\text{C}$ and high light conditions but no stable cultivation of *Rhodomonas* sp. was obtained at higher temperatures under the tested conditions. For all tested temperatures, the total biomass production rate increases with increasing light intensities, showing no indications of light inhibition of *Rhodomonas* sp. within the tested light levels ($60\text{--}600 \mu\text{mol m}^{-2} \text{s}^{-1}$). The fatty acid composition and content of the biomass is significantly influenced by temperature only and not by light intensity. Fatty acid composition shows a strong correlation between cultivation temperature and the degree of saturation with a higher degree of saturation found at higher temperatures. The total-fatty acid production rate follows the same pattern as the biomass production rate with a maximum at higher temperatures and high light conditions. The EPA + DHA content, however, has an optimum at $20 \text{ }^{\circ}\text{C}$ at all tested light intensities. These results show that stable production of *Rhodomonas* sp. at high production rates and with high EPA and DHA content is possible under lab scale conditions. The results provide valuable information moving towards large-scale production of this species for aqua feed applications.

CRedit authorship contribution statement

P.C. Oostlander: Conceptualization, Methodology, Writing - review & editing, Investigation, Formal analysis, Writing - original draft. **J. van Houcke:** Conceptualization, Methodology, Writing - review & editing, Supervision. **R.H. Wijffels:** Conceptualization, Methodology, Writing - review & editing, Supervision. **M.J. Barbosa:** Conceptualization, Methodology, Writing - review & editing, Supervision.

Declaration of competing interest

The authors declare that they have no known competing financial interests or personal relationships that could have appeared to influence the work reported in this paper.

Acknowledgements

This study was co-financed by taskforce SIA, part of the Netherlands Organization for Scientific Research (NWO).

Appendix A. Supplementary data

Supplementary data to this article can be found online at <https://doi.org/10.1016/j.algal.2020.101889>.

References

- [1] J.G. Støttrup, J. Jensen, Influence of algal diet on feeding and egg-production of the calanoid copepod *Acartia tonsa* Dana, *J. Exp. Mar. Biol. Ecol.* 141 (1990) 87–105.
- [2] R.M. Knuckey, G.L. Semmens, R.J. Mayer, M.A. Rimmer, Development of an optimal microalgal diet for the culture of the calanoid copepod *Acartia sinjiensis*: effect of algal species and feed concentration on copepod development, *Aquaculture* 249 (2005) 339–351.
- [3] P. Seixas, P. Coutinho, M. Ferreira, A. Otero, Nutritional value of the cryptophyte *Rhodomonas* lens for *Artemia* sp., *J. Exp. Mar. Biol. Ecol.* 381 (2009) 1–9.
- [4] N. Nogueira, B. Sumares, F.A. Nascimento, L. Png-Gonzalez, A. Afonso, Effects of mixed diets on the reproductive success and population growth of cultured *Acartia grani* (Calanoida), *J. Appl. Aquac.* (2019) 1–14.
- [5] R.M. Chaloub, N.M.S. Motta, S.P. de Araujo, P.F. de Aguiar, A.F. da Silva, Combined effects of irradiance, temperature and nitrate concentration on phycoerythrin content in the microalga *Rhodomonas* sp. (Cryptophyceae), *Algal Res.*, 8 (2015) 89–94.
- [6] A. Bartual, L.M. Lubián, F. Gálvez, Effect of Irradiance on Growth, Photosynthesis, Pigment Content and Nutrient Consumption in Dense Cultures of *Rhodomonas salina* (Wisilouch) (Cryptophyceae), (2002).
- [7] M. Guevara, B.O. Arredondo-Vega, Y. Palacios, K. Saéz, P.I. Gómez, Comparison of growth and biochemical parameters of two strains of *Rhodomonas salina* (Cryptophyceae) cultivated under different combinations of irradiance, temperature, and nutrients, *J. Appl. Phycol.*, (2016) 1–10.
- [8] A. Hammer, R. Schumann, H. Schubert, Light and temperature acclimation of *Rhodomonas salina* (Cryptophyceae): photosynthetic performance, *Aquat. Microb. Ecol.* 29 (2002) 287–296.
- [9] C. Thoisen, M.T.T. Vu, T. Carron-Cabaret, P.M. Jepsen, S.L. Nielsen, B.W. Hansen, Small-scale experiments aimed at optimization of large-scale production of the microalga *Rhodomonas salina*, *J. Appl. Phycol.*, 30 (2018) 2193–2202.
- [10] S. Yamamoto, R. Yamato, T. Yoshimatsu, Optimum culture conditions of *Rhodomonas* sp. Hf-1 strain as a live food for aquatic animals, *Fish. Sci.* 84 (2018) 691–697.
- [11] S. Yamamoto, R. Yamato, Y. Aritaki, P. Bossier, T. Yoshimatsu, Development of a culture protocol for *Rhodomonas* sp. Hf-1 strain through laboratory trials, *Fish. Sci.*,

- (2019) 1–9.
- [12] S.M. Renaud, D.L. Parry, L.V. Thinh, C. Kuo, A. Padovan, N. Sammy, Effect of light intensity on the proximate biochemical and fatty-acid composition of *Isochrysis* sp and *Nannochloropsis oculata* for use in tropical aquaculture, *J. Appl. Phycol.*, 3 (1991) 43–53.
- [13] A.F. da Silva, S.O. Lourenço, R.M. Chaloub, Effects of nitrogen starvation on the photosynthetic physiology of a tropical marine microalga *Rhodomonas* sp. (Cryptophyceae), *Aquat. Bot.* 91 (2009) 291–297.
- [14] P. Boelen, A. van Mastrigt, H.H. van de Bovenkamp, H.J. Heeres, A.G. Buma, Growth phase significantly decreases the DHA-to-EPA ratio in marine microalgae, *Aquac. Int.*, 1–11.
- [15] M.T.T. Vu, C. Douët, T.A. Rayner, C. Thoisen, S.L. Nielsen, B.W. Hansen, Optimization of photosynthesis, growth, and biochemical composition of the microalga *Rhodomonas salina*—an established diet for live feed copepods in aquaculture, *J. Appl. Phycol.*, 28 (2016) 1485–1500.
- [16] E. Valenzuela-Espinoza, F. Lafarga-De-La-Cruz, R. Millán-Núñez, F. Núñez-Cebrero, Growth, nutrient uptake and proximate composition of *Rhodomonas* sp. cultured using f/2 medium and agricultural fertilizers, *Cienc. Mar.* 31 (2005) 79–89.
- [17] F. Lafarga-De la Cruz, E. Valenzuela-Espinoza, R. Millán-Núñez, C.C. Trees, E. Santamaría-del-Ángel, F. Núñez-Cebrero, Nutrient uptake, chlorophyll a and carbon fixation by *Rhodomonas* sp.(Cryptophyceae) cultured at different irradiance and nutrient concentrations, *Aquac. Eng.*, 35 (2006) 51–60.
- [18] C.V. Thoisen, Roskilde Universitet (Ed.), Optimizing the Cultivation of the Cryptophyte *Rhodomonas Salina* for Aquaculture, 2018.
- [19] M.T.T. Vu, P.M. Jepsen, N.O. Jørgensen, B.W. Hansen, S.L. Nielsen, Testing the yield of a pilot-scale bubble column photobioreactor for cultivation of the microalga *Rhodomonas salina* as feed for intensive calanoid copepod cultures, *Aquac. Res.*, 50 (2019) 63–71.
- [20] V. Patil, T. Kallqvist, E. Olsen, G. Vogt, H.R. Gislerod, Fatty acid composition of 12 microalgae for possible use in aquaculture feed, *Aquac. Int.*, 15 (2007) 1–9.
- [21] J.H. de Vree, R. Bosma, R. Wieggers, S. Gegic, M. Janssen, M.J. Barbosa, R.H. Wijffels, Turbidostat operation of outdoor pilot-scale photobioreactors, *Algal Res.*, 18 (2016) 198–208.
- [22] J.H. De Vree, R. Bosma, M. Janssen, M.J. Barbosa, R.H. Wijffels, Comparison of four outdoor pilot-scale photobioreactors, *Biotechnology for biofuels*, 8 (2015) 215.
- [23] F.G. Ación, J.M. Fernández, J.J. Magán, E. Molina, Production cost of a real microalgae production plant and strategies to reduce it, *Biotechnol. Adv.* 30 (2012) 1344–1353.
- [24] R. Guillard, P. Hargraves, *Stichochrysis immobilis* is a diatom, not a chrysophyte, *Phycologia* 32 (1993) 234–236.
- [25] L. De Winter, I. Cabanelas, A. Órfão, E. Vaessen, D. Martens, R. Wijffels, M. Barbosa, The influence of day length on circadian rhythms of *Neochloris oleoabundans*, *Algal Res.*, 22 (2017) 31–38.
- [26] G.M. León-Saiki, I.M. Remmers, D.E. Martens, P.P. Lamers, R.H. Wijffels, D. van der Veen, The role of starch as transient energy buffer in synchronized microalgal growth in *Acutodesmus obliquus*, *Algal Res.*, 25 (2017) 160–167.
- [27] G. Breuer, W.A. Evers, J.H. de Vree, D.M. Kleinegris, D.E. Martens, R.H. Wijffels, P. Lamers, Analysis of fatty acid content and composition in microalgae, *J. Vis. Exp.*, (2013).
- [28] S.M. Renaud, L.-V. Thinh, G. Lambrinidis, D.L. Parry, Effect of temperature on growth, chemical composition and fatty acid composition of tropical Australian microalgae grown in batch cultures, *Aquaculture* 211 (2002) 195–214.
- [29] S.M. Renaud, L.-V. Thinh, G. Lambrinidis, D.L. Parry, Effect of temperature on growth, chemical composition and fatty acid composition of tropical Australian microalgae grown in batch cultures, *Aquaculture* 211 (2002) 195–214.
- [30] A. Taleb, J. Pruvost, J. Legrand, H. Marec, B. Le-Gouic, B. Mirabella, B. Legeret, S. Bouvet, G. Peltier, Y. Li-Beisson, Development and validation of a screening procedure of microalgae for biodiesel production: application to the genus of marine microalgae *Nannochloropsis*, *Bioresour. Technol.*, 177 (2015) 224–232.
- [31] M.H.A. Michels, P.M. Slegers, M.H. Vermeu, R.H. Wijffels, Effect of biomass concentration on the productivity of *Tetraselmis suecica* in a pilot-scale tubular photobioreactor using natural sunlight, *Algal Res.* 4 (2014) 12–18.
- [32] P. Steinrücken, S.K. Prestegard, J.H. de Vree, J.E. Storesund, B. Pree, S.A. Mjøs, S.R. Erga, Comparing EPA production and fatty acid profiles of three *Phaeodactylum tricornutum* strains under western Norwegian climate conditions, *Algal Res.*, 30 (2018) 11–22.
- [33] D.O. Hall, F.G. Acien-Fernandez, E.C. Guerrero, K.K. Rao, E.M. Grima, Outdoor helical tubular photobioreactors for microalgal production: modeling of fluid-dynamics and mass transfer and assessment of biomass productivity, *Biotechnol. Bioeng.*, 82 (2003) 62–73.
- [34] I.M. Remmers, S. D'Adamo, D.E. Martens, R.C. de Vos, R. Mumm, A.H. America, J. H. Cordewener, L.V. Bakker, S.A. Peters, R.H. Wijffels, Orchestration of transcriptome, proteome and metabolome in the diatom *Phaeodactylum tricornutum* during nitrogen limitation, *Algal Res.*, 35 (2018) 33–49.
- [35] J. Liu, M. Sommerfeld, Q. Hu, Screening and Characterization of *Isochrysis* Strains and Optimization of Culture Conditions for Docosahexaenoic Acid Production, (2013), pp. 1–14.
- [36] L. de Winter, I.T.D. Cabanelas, D.E. Martens, R.H. Wijffels, M.J. Barbosa, The influence of day/night cycles on biomass yield and composition of *Neochloris oleoabundans*, *Biotechnology for biofuels*, 10 (2017) 104.
- [37] T. Fernandes, I. Fernandes, C.A. Andrade, N. Cordeiro, Changes in fatty acid biosynthesis in marine microalgae as a response to medium nutrient availability, *Algal Res.* 18 (2016) 314–320.
- [38] T. Fernandes, I. Fernandes, C.A. Andrade, N. Cordeiro, Marine microalgae growth and carbon partitioning as a function of nutrient availability, *Bioresour. Technol.* 214 (2016) 541–547.
- [39] J. van Houcke, I. Medina, H.K. Maehre, J. Cornet, M. Cardinal, J. Linssen, J. Luten, The effect of algae diets (*Skeletonema costatum* and *Rhodomonas baltica*) on the biochemical composition and sensory characteristics of Pacific cupped oysters (*Crassostrea gigas*) during land-based refinement, *Food Res. Int.*, 100 (2017) 151–160.
- [40] R. Huerlimann, R. de Nys, K. Heimann, Growth, lipid content, productivity, and fatty acid composition of tropical microalgae for scale-up production, *Biotechnol. Bioeng.* 107 (2010) 245–257.
- [41] T. Sakamoto, S. Higashi, H. Wada, N. Murata, D.A. Bryant, Low-temperature-induced desaturation of fatty acids and expression of desaturase genes in the cyanobacterium *Synechococcus* sp. PCC 7002, *FEMS Microbiol. Lett.*, 152 (1997) 313–320.
- [42] M. Mitra, S.K. Patidar, S. Mishra, Integrated process of two stage cultivation of *Nannochloropsis* sp. for nutraceutically valuable eicosapentaenoic acid along with biodiesel, *Bioresour. Technol.* 193 (2015) 363–369.
- [43] X. Ma, L. Zhang, B. Zhu, K. Pan, S. Li, G. Yang, Low-temperature affected LC-PUFA conversion and associated gene transcript level in *Nannochloropsis oculata* CS-179, *J. Ocean Univ. China*, 10 (2011) 270–274.
- [44] S. Renaud, H. Zhou, D. Parry, L.-V. Thinh, K. Woo, Effect of temperature on the growth, total lipid content and fatty acid composition of recently isolated tropical microalgae *Isochrysis* sp., *Nitzschia closterium*, *Nitzschia paleacea*, and commercial species *Isochrysis* sp.(clone T. ISO), *J. Appl. Phycol.*, 7 (1995) 595–602.
- [45] C. Zhu, Y. Lee, T. Chao, Effects of temperature and growth phase on lipid and biochemical composition of *Isochrysis galbana* TK1, *J. Appl. Phycol.* 9 (1997) 451–457.
- [46] J. Aussant, F. Guihéneuf, D.B. Stengel, Impact of temperature on fatty acid composition and nutritional value in eight species of microalgae, *Appl. Microbiol. Biotechnol.* 102 (2018) 5279–5297.
- [47] M. Hoffmann, K. Marxen, R. Schulz, K.H. Vanselow, TFA and EPA productivities of *Nannochloropsis salina* influenced by temperature and nitrate stimuli in turbidostat controlled experiments, *Mar. Drugs* 8 (2010) 2526–2545.
- [48] P. Boelen, R. van Dijk, J.S.S. Damsté, W.I.C. Rijpstra, A.G. Buma, On the potential application of polar and temperate marine microalgae for EPA and DHA production, *AMB Express*, 3 (2013) 26.